Acta Crystallographica Section D
Biological Crystallography
ISSN 0907-4449

ADP-2Ho as a phasing tool for nucleotide-containing proteins

Shao-Yang Ku,[a,b] G. David Smith[a] and P. Lynne Howell[a,b]*

[a]Program in Molecular Structure and Function, Research Institute, Hospital for Sick Children, 555 University Avenue, Toronto, Ontario M5G 1X8, Canada, and [b]Department of Biochemistry, Faculty of Medicine, University of Toronto, Toronto, Ontario M5S 1A8, Canada

Correspondence e-mail: howell@sickkids.ca

Received 13 December 2006
Accepted 7 February 2007

PDB Reference: MTR kinase–ADP-2Ho complex, 2olc, r2olcsf.

Trivalent holmium ions were shown to isomorphously replace magnesium ions to form an ADP-2Ho complex in the nucleotide-binding domain of *Bacillus subtilis* 5-methylthioribose (MTR) kinase. This nucleotide–holmium complex provided sufficient phasing power to allow SAD and SIRAS phasing of this previously unknown structure using the $L_{\rm III}$ absorption edge of holmium. The structure of ADP-2Ho reveals that the two Ho ions are approximately 4 Å apart and are likely to share their ligands: the phosphoryl O atoms of ADP and a water molecule. The structure determination of MTR kinase using data collected using Cu $K\alpha$ X-radiation was also attempted. Although the heavy-atom substructure determination was successful, interpretation of the map was more challenging. The isomorphous substitution of holmium for magnesium in the MTR kinase–nucleotide complex suggests that this could be a useful phasing tool for other metal-dependent nucleotide-containing proteins.

1. Introduction

In the absence of a highly similar structural homolog, the incorporation of heavy atoms is the most common way to obtain the crystallographic phases for macromolecular structure determination. While the native S atoms of a protein can sometimes serve as heavy atoms (Lemke *et al.*, 2002; Debreczeni *et al.*, 2003; Ramagopal *et al.*, 2003), the success of sulfur phasing frequently requires superior crystal diffraction quality that is not always obtainable. To circumvent the tedious trial-and-error process of searching for a heavy-atom derivative, more rational approaches are commonly employed. Such methods include metal substitutions for metalloproteins and incorporation of selenomethionine (SeMet; Hendrickson *et al.*, 1990) and occasionally selenotryptophan (Bae *et al.*, 2001; Boles *et al.*, 2002). Although the SeMet method is currently the most popular technique of introducing phasing atoms into a protein, the production of SeMet proteins is not always feasible for proteins produced from nonbacterial expression systems or for proteins purified from native hosts. Furthermore, some proteins simply have an insufficient methionine content to produce sufficient phasing power.

Lanthanide ions are of great interest for crystallographic phasing purposes because of their intense white lines and strong anomalous scattering. These characteristics provide large anomalous signals using single or multiple anomalous dispersion (SAD or MAD; Girard, Anelli *et al.*, 2003; Girard, Stelter, Anelli *et al.*, 2003; Girard, Stelter, Vicat *et al.*, 2003; Purdy *et al.*, 2002) and potentially even larger isomorphous

Table 1
Data-reduction statistics for the ADP-2Ho and ADP-2Mg complexes of *B. subtilis* MTR kinase.

Values in parentheses are for the highest resolution shell.

	ADP-2Ho I	ADP-2Ho II	ADP-2Mg
Space group	$P2_12_12$	$P2_12_12$	$P2_12_12$
Unit-cell parameters (Å)			
a	214.5	215.2	213.8
b	83.5	83.6	83.5
c	51.6	51.6	51.2
Wavelength (Å)	1.5362	1.5418	1.5418
Resolution† (Å)	2.5 (2.61–2.52)	2.0 (2.07–2.00)	2.2 (2.28–2.20)
$R_{\rm merge}$† (%)	10.1 (26.7)	9.3 (43.4)	8.0 (30.2)
Completeness (%)	99.3 (99.6)	98.8 (97.5)	97.5 (96.1)
$\langle I\rangle/\sigma(I)$	46.6 (9.9)	21.9 (9.2)	14.4 (6.2)
Average redundancy	7.3 (5.6)	26.9 (26.6)	13.7 (12.7)

† $R_{\rm merge} = \sum\sum|I(k) - \langle I\rangle|/\sum I(k)$, where $I(k)$ and $\langle I\rangle$ represent the diffraction intensity values of the individual measurements and the corresponding mean values. The summation is over all unique measurements with Friedel pairs merged.

signals using single isomorphous replacement (SIR) or SIR combined with anomalous scattering (SIRAS). Lanthanide derivatives can be prepared by engineering a lanthanide-binding tag (Nitz *et al.*, 2004), although this has not yet been shown to be fruitful for crystallographic phasing owing to the mobility of the tag, or by substituting common metal cofactors, particularly Ca^{II}, with a trivalent lanthanide ion. Trivalent holmium ions (Ho^{III}) have been used to replace Ca^{II} in a calcium-dependent lectin domain from a mannose-binding protein solved by MAD (Weis *et al.*, 1991) as well as in the calcium-binding protein psoriasin solved by MAD (Brodersen *et al.*, 1998) and subsequently by SAD (Brodersen *et al.*, 2000).

In this paper, we show that Ho^{III} can isomorphously replace Mg^{II} to form an ADP-2Ho complex in the nucleotide-binding domain of 5-methylthioribose (MTR) kinase. MTR kinase is a key enzyme in the bacterial methionine-recycling pathway, where it catalyzes the ATP-dependent phosphorylation of MTR to form MTR 1-phosphate. Perhaps owing to its biological role in methionine recycling, many MTR kinases contain less than the expected distribution of methionine. For example, MTR kinase in *Bacillus subtilis* has only two internal methionines in 397 residues, thereby preventing the use of the common SeMet-incorporation method for phasing. The structure of this protein was therefore solved by MAD at the $L_{\rm III}$ absorption edge of holmium using the ADP-2Ho complex. The analysis of this newly determined structure and its function will be discussed in detail elsewhere (Ku *et al.*, in preparation). Here, we focus on the structure of the ADP-2Ho nucleotide in MTR kinase and the use of holmium as a phasing derivative. The ADP-2Ho data have sufficient anomalous signal to allow SAD phasing, but insufficient isomorphous phasing power when combined with the ADP-2Mg data. Structural comparison, however, suggests that the ADP-2Ho and ADP-2Mg MTR kinase complexes are isomorphous. Thus, we propose that ADP-2Ho structurally mimics nucleotides in complex with Mg^{II} or Mn^{II} and hence could serve as a convenient and powerful phasing derivative to aid in the structure determination of a wide spectrum of metal-dependent nucleotide-binding proteins.

2. Methods and results

2.1. Expression, purification, crystallization and preparation of ADP-2Ho and ADP-2Mg complexes of *B. subtilis* MTR kinase

B. subtilis MTR kinase was expressed, purified and crystallized as described previously (Ku *et al.*, 2004). The crystals were grown from 22%(*w*/*v*) PEG 2000 MME, 0.1 *M* Tris–HCl pH 7.5 and 0.3 *M* sodium acetate. The nucleotide complexes of the enzyme were prepared by soaking the crystals for 3 d by adding 2 µl of a soaking solution consisting of 25%(*w*/*v*) PEG 2K MME, 0.1 *M* Tris–HCl pH 7.5, 0.3 *M* sodium acetate, 4 m*M* ADP (sodium salt) and 20 m*M* magnesium acetate to the crystallization drop. The ADP-2Ho complex was prepared in a similar manner. A solution consisting of 25%(*w*/*v*) PEG 2K MME, 0.1 *M* Tris–HCl pH 7.5, 0.3 *M* sodium acetate, 10 m*M* ADP (sodium salt) and holmium chloride ($HoCl_3$) at an initial concentration of 20 m*M* was prepared. Some white gelatinous precipitate was observed in the buffer. The precipitate was spun down in a bench centrifuge for 30 s and 2 µl supernatant was added to the crystals. The crystals were soaked for 3–5 d prior to data collection. Although we attempted to cocrystallize *B. subtilis* MTR kinase with ADP-2Ho, no crystals were obtained. This is probably owing to the precipitation of the holmium phosphate and ADP salts interfering with the crystal nucleation and crystal growth.

2.2. Data collection of ADP-2Ho and ADP-2Mg complexes of *B. subtilis* MTR kinase

Prior to data collection, all crystals of *B. subtilis* MTR kinase were soaked in a cryoprotectant consisting of 25%(*w*/*v*) PEG 2K MME, 0.1 *M* Tris–HCl pH 7.5, 0.3 *M* sodium acetate and 25%(*v*/*v*) ethylene glycol for 10 s and then flash-frozen in a cold stream at 110 K. Three complete data sets were collected: one from a crystal of the ADP-2Mg complex and two from crystals of the ADP-2Ho complex. The first ADP-2Ho data set (ADP-2Ho I) was collected to 2.5 Å resolution

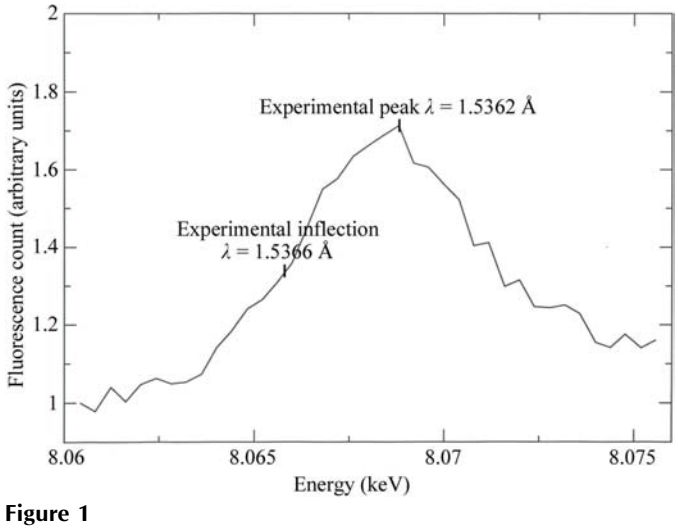

Figure 1
Fluorescence scan of the *B. subtilis* MTR kinase–ADP-2Ho complex at the Ho $L_{\rm III}$ edge.

on an ADSC Quantum 4R CCD detector using synchrotron radiation at a wavelength of 1.5362 Å (Ho L_{III} absorption peak; Fig. 1) from an Si(111) monochromator having a bandwidth of 2 eV at beamline X8C, National Synchrotron Light Source, Brookhaven National Laboratory. The second ADP-2Ho data set (ADP-2Ho II) was collected to 2.0 Å resolution with higher redundancy on an R-AXIS IV^{++} image-plate detector using Cu $K\alpha$ X-ray radiation from an RU-H3R rotating-anode generator. The data from the ADP-2Mg complex were also collected on our home source to 2.1 Å resolution. All crystals of *B. subtilis* MTR kinase belong to space group $P2_12_12$ and contain two monomers per asymmetric unit. The synchrotron data were processed using *HKL-2000* (Otwinowski & Minor, 1997), while those collected at home were processed using *d*TREK* (Pflugrath, 1999). Table 1 summarizes the data-reduction statistics.

Table 2
SAD and SIRAS phasing statistics.

	ADP-2Ho I SAD	ADP-2Ho I/ ADP-2Mg SIRAS	ADP-2Ho II SAD	ADP-2Ho II/ ADP-2Mg SIRAS
SHELXD				
CC(all)†	59.72	57.65	29.9‡	24.86‡
CC(weak)†	41.54	47.49	16.6‡	15.22‡
SHELXE				
Contrast§	0.55 (0.43)	0.58 (0.42)	0.56 (0.50)	0.58 (0.50)
Connectivity§	0.90 (0.86)	0.93 (0.86)	0.86 (0.84)	0.90 (0.84)
Pseudo-free CC§ (%)	69.0 (62.8)	65.3 (58.1)	54.8 (56.7)	58.7 (56.7)

† Correlation coefficient CC between E_{obs} and E_{calc}. CC(all) values were calculated for all E values, whilst CC(weak) was only for those E values not used directly for substructure solution (Schneider & Sheldrick, 2002). ‡ Although the CC(all)/CC(weak) values are smaller than the borderline values of 30/15 for a structure considered to be solved by *SHELXD*, the final Ho substructure solutions are correct. § Contrast, connectivity and pseudo-free CC are defined in *SHELXE* (Sheldrick, 2002). As expected, these values are higher for the correct enantiomorph than those for the inverted substructure (values in parentheses), with the exception of the pseudo-free CC for SAD phasing using the ADP-2Ho II data. Since the F_o map calculated from these phases does not clearly differentiate the correct enantiomorph, only the SIRAS map is presented in Fig. 2 for the ADP-2Ho II data.

2.3. SAD and SIRAS phasing of *B. subtilis* MTR kinase using holmium

The anomalous substructures for both holmium data sets were determined using the Bijvoet differences (*i.e.* SAD) using the program *SHELXD* (Schneider & Sheldrick, 2002). The holmium substructures determined based on the intensity differences between the holmium and the magnesium complexes in conjunction with the anomalous difference of the holmium (*i.e.* SIRAS) were also solved using *SHELXD*. All substructure solutions

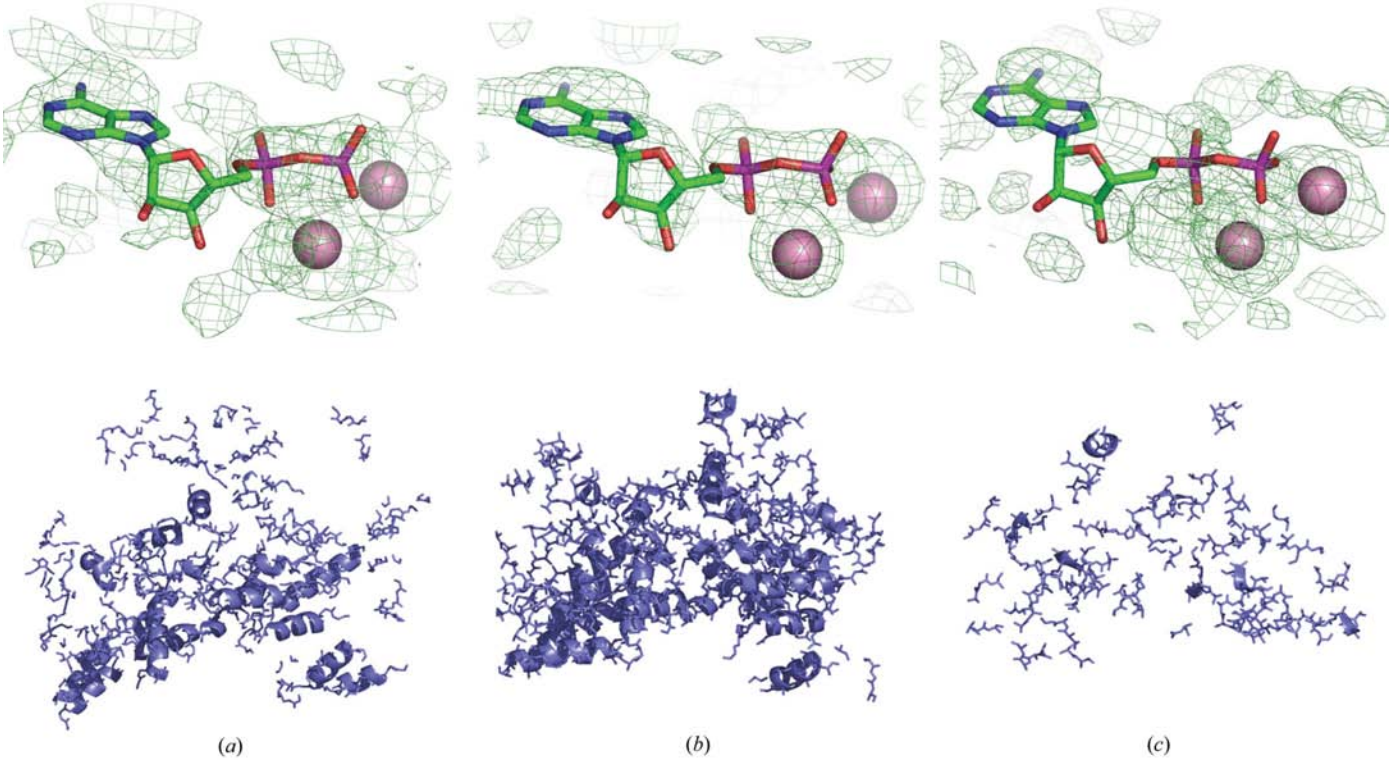

Figure 2
F_o maps and the initial *RESOLVE* models with (*a*) SAD, (*b*) ADP-2Ho I SIRAS and (*c*) ADP-2Ho II SIRAS phases. The F_o maps in lime are contoured at 1σ with the refined model of ADP-2Ho superimposed for reference. The backbone atoms of the *RESOLVE* models are shown as dark blue sticks with helices highlighted in cartoon representation. The *RESOLVE* models for (*a*) the SAD and (*b*) the SIRAS phases from synchrotron radiation and (*c*) the SIRAS phases from the Cu $K\alpha$ radiation source are about 50, 47 and 16% complete, respectively. Although more residues were built into the SAD map in (*a*), the resulting *RESOLVE* model has a poorer secondary-structure profile than the SIRAS model in (*b*). This figure was prepared using *PyMOL* (DeLano, 2002).

were compared and shown to be identical after correcting for permissible origins, the enantiomorph and crystallographic symmetry using the program *NANTMRF* (Smith, 2002). Four holmium sites were found to be consistent across all of the substructures: namely, four holmium ions per asymmetric unit or two holmium ions per MTR kinase monomer. The SAD and SIRAS phasing and density modification without noncrystallographic symmetry (NCS) averaging were performed using *SHELXE* (Sheldrick, 2002). All *SHELXE* jobs were run for 20 cycles with a solvent content of 0.45. The *SHELXD* and *SHELXE* phasing statistics are summarized in Table 2.

For the synchrotron-radiation ADP-2Ho I data, the F_o electron-density maps phased by either HoSAD or HoSIRAS were of good quality and allowed autotracing of the protein at 2.5 Å using *RESOLVE* (Terwilliger & Berendzen, 1999; Terwilliger, 2000; Figs. 2*a* and 2*b*). In the F_o maps, unambiguous density for an ADP molecule was found in the protein's active site and two holmium ions were located near the phosphoryl groups of the ADP molecule. However, the ADP-2Ho II data set, despite its higher resolution and redundancy than the ADP-2Ho I data, resulted in electron-density maps of poorer quality. Only the SIRAS map is shown in Fig. 2(*c*) because subsequent analysis showed that while the anomalous signal was capable of determining the substructure, the subsequent SAD map was incapable of determining the correct enantiomorph (Table 2). The anomalous signal is masked by experimental errors beyond 5 Å resolution (see below). The *RESOLVE* models for the SAD, SIRAS (ADP-2Ho I data) and SIRAS (ADP-2Ho II data) phases are approximately 50, 47 and 16% complete, respectively.

2.4. Structure refinement of the ADP-2Ho complex

Structure refinement of the ADP-2Ho complex was alternated between *CNS* (Brünger *et al.*, 1998) and manual modeling using *Coot* (Emsley & Cowtan, 2004) with phased-combined σ_A-weighted $2F_o - F_c$ and $F_o - F_c$ maps using the 2.0 Å ADP-2Ho II data. Initial refinement procedures consisted of rigid-body refinement, torsion-angle simulated annealing using a maximum-likelihood (ML) experimental amplitude distribution (MLF) and grouped *B*-factor refinement. All refinements were monitored by the improvement of R_{free} (Brünger, 1993) with 5% cross-validated data. NCS restraints were imposed between the two monomers in the asymmetric unit until there was no further improvement in R_{free}. The final model for *B. subtilis* MTR kinase in complex with ADP-2Ho is a dimer consisting of residues 5–26, 32–51, 56–66 and 74–396 for monomer *A* and residues 7–29, 32–50,

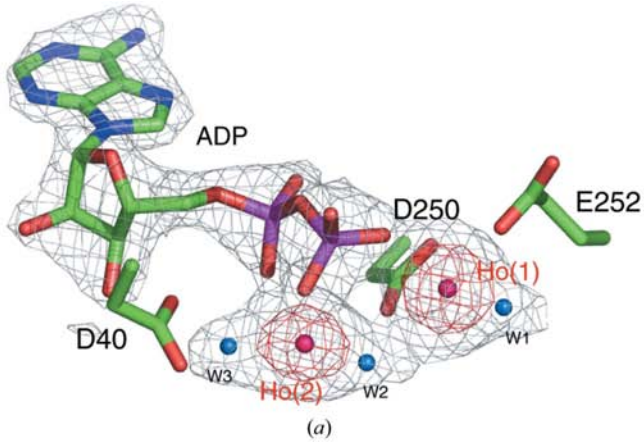

(*a*)

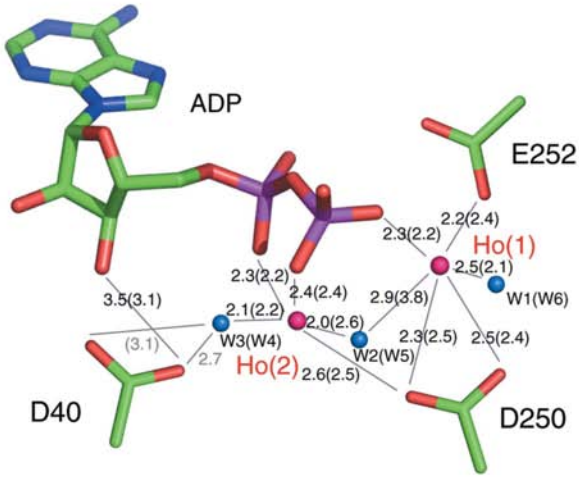

(*b*)

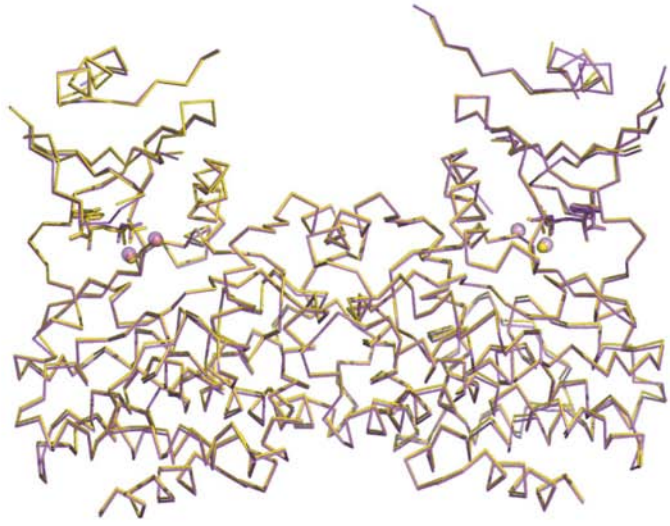

(*c*)

Figure 3
The ADP-2Ho-binding site of *B. subtilis* MTR kinase. (*a*) Three-dimensional structure of the ADP-2Ho-binding site. The electron density in gray and red is the σ_A-weighted $F_o - F_c$ ADP-2Ho and water OMIT map contoured at 3σ and 15σ, respectively. (*b*) A schematic diagram showing the interactions between the holmium ions and the protein. The bond distances, given in Å, refer to those in monomer *A*; the values in parentheses refer to the distance in monomer *B*. Values in gray are the interactions that differ between the two monomers of the protein. In (*a*) and (*b*), the nucleotide and protein residues are presented as sticks, with C, N, O and P atoms coloured green, blue, red and magenta, respectively. The Ho ions are shown as magenta spheres and water molecules as blue spheres. (*c*) C^{α} superimposition of the MTR kinase ADP-2Ho complex (pink) and the ADP-2Mg complex (yellow; Ku *et al.*, in preparation). The Ho ions are displayed as pink spheres and the Mg ions as yellow spheres. The radii of the spheres are drawn to approximate the ionic radii of the ions (Ho^{III}, 0.90 Å; Mg^{II}, 0.72 Å). This figure was prepared using *PyMOL* (DeLano, 2002).

56–67 and 75–396 for monomer *B*. The N-terminal domain (residues 1–120) is more disordered than the C-terminal domain (residues 121–397). The density for the side chains of some residues was insufficient to allow the side chains to be modeled and hence these residues have been truncated to alanine. The side chains of the following residues have been omitted: residues 5, 7, 8, 10, 20, 23, 36, 56, 66, 108, 190, 196, 197, 302, 305, 306, 314, 316 and 369 in monomer *A*, and residues 8, 10, 23, 26, 29, 36, 42, 56, 66, 108, 138, 190, 298, 302, 306 and 382 in monomer *B*. Each monomer of the protein contains one ADP molecule and two holmium ions. Near each pair of holmium ions, three regions of satellite density were observed at 3σ in the $F_o - F_c$ water OMIT map. Three water molecules were therefore modeled for each ADP-2Ho (W1–3 for monomer *A* and W4–6 for monomer *B*; see below). A CHAPS detergent molecule that facilitates crystal packing was modeled at the crystallographic interface between the C-termini of monomers *A* and *B*. The final round of refinement was performed using *REFMAC* (Murshudov, 1997) with TLS refinement (Winn *et al.*, 2001, 2003). Each domain of MTR kinase was defined as a TLS group (residues 1–120 and 121–397). The final model has an *R* factor of 21.4% and an R_{free} of 25.0%. The crystallographic refinement statistics are summarized in Table 3.

Table 3
Refinement statistics for the *B. subtilis* MTR kinase ADP-2Ho complex refined using ADP-2Ho II data.

Resolution (Å)	2.0
No. of reflections (working set/test set)	60025/3148
No. of atoms (protein/ligand)	6354/89
No. of water molecules	434
R_{cryst}/R_{free}† (%)	21.4/25.0
R.m.s.d. from ideal values	
Bond lengths (Å)	0.010
Bond angles (°)	1.3
Average *B* factor (Å^2)	
Monomer *A*	27.3
N-lobe (1–125)	33.8
C-lobe (126–397)	24.9
ADP	27.6
2Ho	42.0
Waters W1–3	20.8
Monomer *B*	27.1
N-lobe (1–125)	33.6
C-lobe (126–397)	24.7
ADP	29.3
2Ho	40.1
Waters W4–6	23.6
Ramachandran plot‡	
Total favored (%)	97.6
Total allowed (%)	99.6
DPI§ based on R_{free} (Å)	0.17

† $R_{cryst} = \sum |F_{obs} - F_{calc}| / \sum |F_{obs}|$; R_{free} is R_{cryst} for the 5% cross-validated test data. ‡ According to the Ramachandran plot in *MolProbity* (Lovell *et al.*, 2003). § Cruickshank's diffraction-component precision index (DPI; Cruickshank, 1999) as an estimate of coordinate error.

3. Discussion

3.1. ADP-2Ho binding

During the Ho substructure determinations, four Ho ions were found in the asymmetric unit: two in each monomer of MTR kinase. The two Ho ions in each pair were found to be about 4 Å apart. The density-modified F_o and the $2F_o - F_c$ ligand OMIT maps both show that the two Ho ions are in complex with ADP, forming a holmium–ADP complex (ADP-2Ho) with MTR kinase (Figs. 2 and 3*a*). Literature searches and queries of the Cambridge Structural Database (CSD; Allen & Taylor, 2004) reveal no record of a holmium–nucleotide complex of any sort, suggesting that the structure of ADP-2Ho has not been described previously. In the complex, the first holmium ion, Ho(1), is coordinated by the $O^{\delta1}$ and $O^{\delta2}$ carboxyl O atoms of Asp250, the carboxyl $O^{\varepsilon1}$ atom of Glu252, the β phosphoryl O atom of ADP, a singly coordinated water molecule (W1 in monomer *A* and W6 in monomer *B*) and a second water molecule (W2 in monomer *A* and W5 in monomer *B*). In monomer *A*, this water molecule (W2) also coordinates the second holmium, Ho(2). In addition to this shared water molecule, Ho(2) interacts with the α and β phosphoryl O atoms of ADP, the $O^{\delta2}$ atom of Asp250 and a singly coordinated water molecule (W3 and W4 in monomers *A* and *B*, respectively). This water potentially interacts with one of the carboxyl O^{δ} atoms of Asp40. However, owing to poor side-chain density for Asp40, the interaction between W3 or W4 and Asp40 is not consistent between the two monomers of MTR kinase (Fig. 3*b*).

In the *B. subtilis* ADP-2Ho–MTR kinase structure, the interatomic distance between the two Ho ions is 4.1 and 3.9 Å for monomers *A* and *B*, respectively. Since a $HoCl_3$ solution was used to derivatize the protein, the bound Ho ions are assumed to be trivalent. Because of potential electrostatic repulsion, a distance of 4 Å between two trivalent holmium ions may seem to be unusually short, but not when O atoms bridge the metal ions. A search of the CSD (Allen & Taylor, 2004) reveals two dinuclear holmium compounds with interatomic distances between the two Ho ions of 4 Å or shorter: tetraqua-bis(μ_2-hydroxo)-tetrakis(1,10-phenanthroline)-diholmium tetraperchlorate 1,10-phenanthroline solvate (Bukietynska *et al.*, 1989) and aqua-tris(μ_2-*N*,*N*′-di-isonicotinoyl-2-oxy-5-methylisophthalaldehyde dihydrazone)-holmium(III) dinitrate hydroxide hydrate (Bu *et al.*, 2000). The distances between the holmium ions in these structures are 3.67 and 3.54 Å, respectively. In both compounds, the diholmium ions are bridged by hydroxyl O atoms. In the structure of the ADP-2Ho complex, the two Ho ions likely share some of their coordinating ligands: the phosphoryl O atoms of ADP, Asp250 $O^{\delta2}$ and a water molecule.

While an alternative explanation for the short distance separating the two positively charged Ho^{III} ions is that each Ho_{III} site is only half occupied, this appears to be less likely, as the occupancies of the Ho ions in the *SHELXD* substructure determinations refined to 1.0. In addition, in the refined structure, while the Ho ions do have a slightly higher *B* factors (~40 Å^2) compared with their neighboring atoms (~25–27 Å^2; Table 2) when the occupancy is fixed at 1.0, refinements fixing the occupancy at 0.5 resulted in *B* factors for the Ho ions of less than 13 Å^2. Calculations suggest that the average occupancy for the Ho ions is 70%. Other metal ions have been

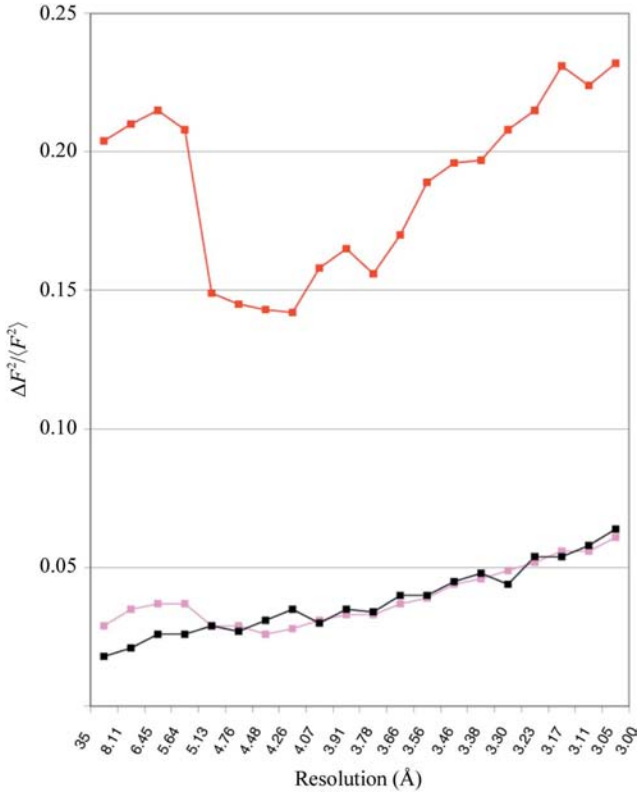

Figure 4
The plot of relative intensity difference *versus* resolution. All data were processed using the program *BAYES* (French & Wilson, 1978; Blessing *et al.*, 1998) and scaled using the program *DATANAL*, which minimizes either $\Delta F^2/\langle F^2\rangle$ or $\Delta F^2/\sigma(\Delta F^2)$ using a linear or nonlinear least-square procedure, respectively. Each resolution bin holds an equivalent number of reflections. The red and pink plots are the anomalous differences from 35 to 3.0 Å resolution for the ADP-2Ho I and the ADP-2Ho II data, respectively. The black plot is the intensity difference between the Friedel mates of the ADP-2Mg data. Since no significant anomalous difference is expected, the black plot serves as a reference for the expected errors in $\Delta F^2/\langle F^2\rangle$ as a function of resolution.

observed in close proximity to each other when trapped in a cage of acidic residues, as their positive charges are partially neutralized by their ligands. For example, Ca^{II} ions, which have a larger ionic radius than Ho^{III} in all coordination states (Shannon, 1976), have interatomic distances ranging from 3.8 to 4.1 Å in the multi-calcium-binding bone protein osteocalcin (Hoang *et al.*, 2003).

3.2. ADP-2Ho as a heavy-atom derivative

Holmium has been used previously as a phasing atom: it has been used to replace Ca^{II} in the calcium-dependent lectin domain of a mannose-binding protein (Weis *et al.*, 1991) and in the calcium-binding protein psoriasin (Brodersen *et al.*, 1998, 2000). In the current work, the ADP-2Ho derivative of MTR kinase has large Bijvoet differences and excellent phasing power at the L_{III} absorption edge of holmium, which allowed the *de novo* structure determination of the protein by SAD.

The plot of relative anomalous difference $\Delta F^2/\langle F^2\rangle$ *versus* resolution shows that the anomalous difference at the L_{III} absorption edge of holmium is at least 14% (Fig. 4). A slight increase in the intensity difference is observed around 6 Å resolution because the holmium ions are 'seen' as a binuclear 'superatom' (Fig. 4, red). This characteristic increase in the anomalous difference at 6 Å resolution is also observed in the Cu $K\alpha$ ADP-2Ho II data (Fig. 4, pink). The advantage of anomalous dispersion is that the size of the signal is generally a function of wavelength, not resolution. Thus, the relative contribution of the anomalous signal to the intensity of a reflection should increase with resolution. However, more often than not the anomalous difference is gradually masked by large errors in intensity measurement at higher resolution. The Friedel difference of ADP-2Mg (Fig. 4, black) serves as a control and a reference for the expected errors in $\Delta F^2/\langle F^2\rangle$ as a function of resolution since no anomalous signal is expected from Mg^{II} ions. As expected, *SHELXD* failed to solve the substructure for Mg based on its Friedel differences, but did succeed in solving all the other anomalous and/or isomorphous substructures (Table 2). Theoretical calculations suggests that two holmium ions ($\Delta f'' \simeq 4$ at $\lambda = 1.5418$ Å) would only generate 1.5% anomalous signal for the 397-residue MTR kinase. When compared with the ADP-2Mg reference data, the Cu K^{α} ADP-2Ho II data show little or no anomalous signal contributed by Ho at resolutions higher than 5 Å, suggesting that experimental errors already exceed 1.5% at 5 Å resolution.

Superimposition of the ADP-2Ho and ADP-2Mg (Ku *et al.*, in preparation) MTR kinase structures shows that Ho^{III} has isomorphously replaced Mg^{II} (Fig. 3*c*). The unit-cell parameters differ by less than 0.8% and an *a posteriori* structural comparison of the two structures shows that their C^{α} r.m.s.d. is about 0.4 Å (Fig. 3*c*) and that their entire unit-cell contents can be readily superimposed. The crystals of the ADP-2Mg and ADP-2Ho MTR kinase complexes can therefore be considered to be isomorphous. In theory, the isomorphous difference between the two complexes is 54 electrons per heavy atom (Mg^{II} = 10 e; Ho^{III} = 64 e), which should have resulted in a large isomorphous signal. However, SAD phasing using Cu $K\alpha$ radiation resulted in an uninterpretable map owing to the lack of anomalous signal at resolutions higher than 5 Å and SIRAS phasing did not yield a F_o map that would allow significant autotracing by *RESOLVE* (Fig. 2*c*). Furthermore, the SIRAS and SAD maps were of comparable quality when the synchrotron data were used (Figs. 2*a* and 2*b*). Ravelli *et al.* (2005) demonstrate that systematically exposing a crystal of nitroreductase to radiation damage, which resulted in an increase in R_{merge} from 4.3% to 5.3% (2.0 Å), was sufficient to prevent substructure determination with *SHELXD*. Radiation damage is not observed in the Cu $K\alpha$ ADP-2Ho II data set, as its R_{merge}, χ^2 and scaling factors are consistent throughout all frames. Instead, it would appear that data quality of the MTR kinase crystals, all of which have R_{merge} in the 8–10% range, has undermined the weak signal obtainable from the Cu $K\alpha$ X-ray source and prevented successful structure determination.

Although synchrotron radiation was required for the structure determination of *B. subtilis* MTR kinase, ADP-2Ho proved to be a convenient and powerful phasing derivative

and in cases where more accurate data can be collected may also prove useful for Cu $K\alpha$ data. This idea is supported by computational studies of Mg^{II} substitution by trivalent lanthanum cations (La^{III}) in proteins, which show that La^{III} can favorably substitute for Mg^{II} in mononuclear and binuclear Mg^{II}-binding sites if sufficient carboxylate groups are available (Dudev *et al.*, 2005). Most nucleotide–Mg^{II}-binding proteins have at least one aspartate and/or glutamate residue in addition to the phosphoryl O atoms from the nucleotide in their active sites. Furthermore, during the structure determination of the RhoA–RhoGDI (Ras homology protein–guanine nucleotide-exchange inhibitor) complex, holmium was used as a heavy-atom derivative. A single Ho^{III} ion was found near the β phosphate of GDP in the active site, possibly replacing the Mg^{II} in GDP-Mg (Longenecker *et al.*, 1999). Thus, we propose that ADP-2Ho and potentially other nucleotide–2Ho complexes may be able to aid the *de novo* structure determination of a wide spectrum of metal-dependent nucleotide-binding proteins.

This work was supported by a research grant from the Canadian Institutes of Health Research (No. 43998). PLH and S-YK are the recipients of a Canada Research Chair in Structural Biology and a Natural Sciences and Engineering Research Council of Canada postgraduate scholarship, respectively. Station X8C at National Synchrotron Light Source, Brookhaven National Laboratory is supported by the United States Department of Energy and Multi-User maintenance grants from the Canada Institutes of Health Research and the Natural Sciences and Engineering Research Council of Canada.

References

Allen, F. H. & Taylor, R. (2004). *Chem. Soc. Rev.* **33**, 463–475.
Bae, J. H., Alefelder, S., Kaiser, J. T., Friedrich, R., Moroder, L., Huber, R. & Budisa, N. (2001). *J. Mol. Biol.* **309**, 925–936.
Blessing, R. H., Guo, D. Y. & Langs, D. A. (1998). *Direct Methods for Solving Macromolecular Structures*, edited by S. Fortier, pp. 47–71. Dordrecht: Kluwer Academic Publishers.
Boles, J. O., Henderson, J., Hatch, D. & Silks, L. A. (2002). *Biochem. Biophys. Res. Commun.* **298**, 257–261.
Brodersen, D. E., de La Fortelle, E., Vonrhein, C., Bricogne, G., Nyborg, J. & Kjeldgaard, M. (2000). *Acta Cryst.* D**56**, 431–441.
Brodersen, D. E., Etzerodt, M., Madsen, P., Celis, J. E., Thogersen, H. C., Nyborg, J. & Kjeldgaard, M. (1998). *Structure*, **6**, 477–489.
Brünger, A. T. (1993). *Acta Cryst.* D**49**, 24–36.
Brünger, A. T., Adams, P. D., Clore, G. M., DeLano, W. L., Gros, P., Grosse-Kunstleve, R. W., Jiang, J.-S., Kuszewski, J., Nilges, M., Pannu, N. S., Read, R. J., Rice, L. M., Simonson, T. & Warren, G. L. (1998). *Acta Cryst.* D**54**, 905–921.
Bu, X. H., Du, M., Zhang, L., Song, X. B., Zhang, R. H. & Clifford, T. (2000). *Inorg. Chim. Acta*, **308**, 143–149.
Bukietyńska, K., Ngoc, T. P. & Starynowicz, P. (1989). *Acta Cryst.* C**45**, 553–556.
Cruickshank, D. W. (1999). *Acta Cryst.* D**55**, 583–601.
Debreczeni, J. É., Bunkoczi, G., Ma, Q., Blaser, H. & Sheldrick, G. M. (2003). *Acta Cryst.* D**59**, 688–696.
DeLano, W. L. (2002). *The PyMOL Molecular Graphics System.* http://www.pymol.org.
Dudev, T., Chang, L. Y. & Lim, C. (2005). *J. Am. Chem. Soc.* **127**, 4091–4103.
Emsley, P. & Cowtan, K. (2004). *Acta Cryst.* D**60**, 2126–2132.
French, S. & Wilson, K. (1978). *Acta Cryst.* A**34**, 517–525.
Girard, E., Anelli, P. L., Vicat, J. & Kahn, R. (2003). *Acta Cryst.* D**59**, 1877–1880.
Girard, E., Stelter, M., Anelli, P. L., Vicat, J. & Kahn, R. (2003). *Acta Cryst.* D**59**, 118–126.
Girard, E., Stelter, M., Vicat, J. & Kahn, R. (2003). *Acta Cryst.* D**59**, 1914–1922.
Hendrickson, W. A., Horton, J. R. & LeMaster, D. M. (1990). *EMBO J.* **9**, 1665–1672.
Hoang, Q. Q., Sicheri, F., Howard, A. J. & Yang, D. S. (2003). *Nature (London)*, **425**, 977–980.
Ku, S. Y., Yip, P., Cornell, K. A., Riscoe, M. K. & Howell, P. L. (2004). *Acta Cryst.* D**60**, 116–119.
Lemke, C. T., Smith, G. D. & Howell, P. L. (2002). *Acta Cryst.* D**58**, 2096–2101.
Longenecker, K., Read, P., Derewenda, U., Dauter, Z., Liu, X., Garrard, S., Walker, L., Somlyo, A. V., Nakamoto, R. K., Somlyo, A. P. & Derewenda, Z. S. (1999). *Acta Cryst.* D**55**, 1503–1515.
Lovell, S. C., Davis, I. W., Arendall, W. B. III, de Bakker, P. I., Word, J. M., Prisant, M. G., Richardson, J. S. & Richardson, D. C. (2003). *Proteins*, **50**, 437–450.
Murshudov, G. N. (1997). *Acta Cryst.* D**53**, 240–255.
Nitz, M., Sherawat, M., Franz, K. J., Peisach, E., Allen, K. N. & Imperiali, B. (2004). *Angew. Chem. Int. Ed. Engl.* **43**, 3682–3685.
Otwinowski, Z. & Minor, W. (1997). *Methods Enzymol.* **276**, 307–326.
Pflugrath, J. W. (1999). *Acta Cryst.* D**55**, 1718–1725.
Purdy, M. D., Ge, P., Chen, J., Selvin, P. R. & Wiener, M. C. (2002). *Acta Cryst.* D**58**, 1111–1117.
Ramagopal, U. A., Dauter, M. & Dauter, Z. (2003). *Acta Cryst.* D**59**, 1020–1027.
Ravelli, R. B., Nanao, M. H., Lovering, A., White, S. & McSweeney, S. (2005). *J. Synchrotron Rad.* **12**, 276–284.
Schneider, T. R. & Sheldrick, G. M. (2002). *Acta Cryst.* D**58**, 1772–1779.
Shannon, R. D. (1976). *Acta Cryst.* A**32**, 751–767.
Sheldrick, G. M. (2002). *Z. Kristallogr.* **217**, 644–650.
Smith, G. D. (2002). *J. Appl. Cryst.* **35**, 368–370.
Terwilliger, T. C. (2000). *Acta Cryst.* D**56**, 965–972.
Terwilliger, T. C. & Berendzen, J. (1999). *Acta Cryst.* D**55**, 849–861.
Weis, W. I., Kahn, R., Fourme, R., Drickamer, K. & Hendrickson, W. A. (1991). *Science*, **254**, 1608–1615.
Winn, M. D., Isupov, M. N. & Murshudov, G. N. (2001). *Acta Cryst.* D**57**, 122–133.
Winn, M. D., Murshudov, G. N. & Papiz, M. Z. (2003). *Methods Enzymol.* **374**, 300–321.